MOLECULAR AND CELLULAR BIOLOGY, Apr. 2001, p. 2790–2801 Vol. 21, No. 8
0270-7306/01/$04.00+0 DOI: 10.1128/MCB.21.8.2790–2801.2001

Two Compound Replication Origins in *Saccharomyces cerevisiae* Contain Redundant Origin Recognition Complex Binding Sites

JAMES F. THEIS AND CAROL S. NEWLON*

Department of Microbiology and Molecular Genetics, UMDNJ-New Jersey Medical School, Newark, New Jersey 07103

Received 19 October 2000/Returned for modification 4 December 2000/Accepted 25 January 2001

While many of the proteins involved in the initiation of DNA replication are conserved between yeasts and metazoans, the structure of the replication origins themselves has appeared to be different. As typified by *ARS1*, replication origins in *Saccharomyces cerevisiae* are <150 bp long and have a simple modular structure, consisting of a single binding site for the origin recognition complex, the replication initiator protein, and one or more accessory sequences. DNA replication initiates from a discrete site. While the important sequences are currently less well defined, metazoan origins appear to be different. These origins are large and appear to be composed of multiple, redundant elements, and replication initiates throughout zones as large as 55 kb. In this report, we characterize two *S. cerevisiae* replication origins, *ARS101* and *ARS310*, which differ from the paradigm. These origins contain multiple, redundant binding sites for the origin recognition complex. Each binding site must be altered to abolish origin function, while the alteration of a single binding site is sufficient to inactivate *ARS1*. This redundant structure may be similar to that seen in metazoan origins.

The replication of eukaryotic chromosomes initiates at multiple origins during each S phase. These DNA replication origins are best understood in the budding yeast *Saccharomyces cerevisiae*, in which they were initially recognized by their ability to promote the autonomous replication of plasmids. For this reason, they are referred to as autonomously replicating sequence (ARS) elements (29, 55). The paradigm *S. cerevisiae* replication origin is *ARS1*. It has a modular structure that spans about 120 bp and includes a small essential region, domain A, and three small accessory sequences, B1, B2, and B3, mutations in which reduce but do not abolish activity (40). Domain A, which encompasses the essential match to the 11-bp ARS consensus sequence (ACS), is the core of the binding site for the *S. cerevisiae* replication initiator protein, the origin recognition complex (ORC). The six-subunit ORC complex also contacts and protects DNA in the B1 element, and some mutations in B1 compromise ORC binding in vitro (3, 37, 50, 52). The B3 element contains a binding site for the transcriptional activator-repressor Abf1p, which can be replaced by the binding sites for the transcriptional regulators Rap1p and Gal4p (40). The precise role of the B2 element has not been defined, although at least one of its functions is likely to be unwinding the DNA duplex to allow entry of the replication machinery (38, 41).

Other well-studied ARS elements, including *ARS307* (49, 57), *ARS305* (30), *ARS121* (62), and the *H4 ARS* (7), seem to fit the *ARS1* paradigm in that they contain a single, essential ACS flanked by a B domain. However, details of the structure of the B domain differ, and some ARS elements also contain stimulatory sequences on the other side of domain A, a region called domain C.

In this paper, we describe our characterization of two ARS elements, *ARS101* and *ARS310*, which differ from the *ARS1* paradigm in that they contain multiple ORC binding sites, all of which must be inactivated to abolish function. Following the precedent established by Hurst and Rivier (31), we will refer to these elements as compound ARS elements to distinguish them from ARS elements that have a single, essential match to the ACS. The occurrence of redundant ORC binding sites is reminiscent of the structure of *Schizosaccharomyces pombe* ARS elements, which appear to contain redundant functional elements (13, 21, 33, 44), and is similar to one model for the initiation zones detected at mammalian origins (reviewed in references 14 and 25).

MATERIALS AND METHODS

Strains. *Escherichia coli* strain DH5α (Life Technologies, Grand Rapids, N.Y.) was used for routine cloning, and strain GM2929 was used to prepare DNA lacking *dam* modification (46). Uracil-containing DNA was prepared from strain CJ236 (36).

S. cerevisiae strain 1C6 (ATCC 201543) was used for plasmid stability assays, which were performed as described previously (57). Strain YP45 (54) was used for the analyses of replication intermediates of *ARS101* and its mutant derivatives. Strain CN31C, which lacks the 30-kb duplication present in strain YP45 of the region that includes *ARS310* and the adjacent Ty element (43, 63; A. Dershowitz and C. S. Newlon, unpublished data and data not shown), was used for analyses of *ARS310* replication intermediates.

All transformations were performed by electroporation (2).

Plasmids. (i) *ARS101*. pLF34 was provided by David Kaback (Dept. of Microbiology and Molecular Genetics, UMDNJ-New Jersey Medical School, Newark, N.J.). The 1.5-kb *Kpn*I-*Bgl*II fragment of pLF34 was cloned into pBS-KS (Stratagene); the 3.0-kb *Fsp*I fragment of this construct was ligated to the 4.7-kb *Fsp*I fragment of pRS326 (57) and the 2.6-kb *Fsp*I fragment of pRS306 (54) to yield yAR8KG and yAR8KG0, respectively. yAR8KG was isolated from *E. coli* strain GM2929; the 650-bp *Eco*RV-*Cla*I fragment was blunted with T4 polymerase (New England Biolabs [NEB]) plus deoxynucleoside triphosphates (dNTPs) (Roche Molecular Biochemicals), *Hin*dIII linkers (NEB) were attached, and the fragment was cloned into pRS326 to yield yAR8VCA, which contains the *Eco*RV-*Cla*I fragment in the same orientation as in yAR8KG. The *Eco*RV-*Cla*I fragment contains nucleotides 159457 to 160108 of the chromosome I sequence. The mutation in the 11 of 11 match to the ACS was made as described by Kunkel (36), and the mutation in the 9 of 11 match was made by fusion PCR (28). The

* Corresponding author. Mailing address: Department of Microbiology and Molecular Genetics, UMDNJ-New Jersey Medical School, 185 South Orange Ave., Newark, NJ 07103. Phone: (973) 972-4227. Fax: (973) 972-3644. E-mail: newlon@umdnj.edu.

11 of 11 match mutation introduces an *Xba*I site, while the 9 of 11 match mutation introduces an *Msc*I site. yAR8CMA (See Fig. 1E) was created by digesting the 9 of 11 match mutant, yAR8VCA-Msc, with *Msc*I plus *Xho*I, blunting with T4 polymerase plus dNTPs, and recircularizing. yAR8XHA (see Fig. 1F) was created by first cloning the 310-bp *Hin*fI-*Hin*dIII fragment of the 11 of 11 match mutant (blunted with T4 polymerase plus dNTPs) into the filled-in *Hin*dIII site of pRS326 and then digesting the resulting plasmid with *Xba*I and recircularizing.

Mutants constructed in the yAR8VCA backbone were transferred to the yAR8KG0 backbone for integration into the chromosome via a two-step process: First, the 630-bp *Pml*I-*Kpn*I fragment of the mutant was ligated to the 4.8-kb *Pml*I-*Kpn*I fragment of yAR8KG0. Next, the 1.5-kb *Nsi*I fragment of the resulting plasmid was ligated to the 4.3-kb *Nsi*I fragment of yAR8KG0. This step transferred the 150-bp *Pml*I-*Nsi*I fragment of the mutant into the yAR8KG0 backbone. Plasmids were linearized by digestion with *Ehe*I to direct integration for two-step gene replacements (6), which resulted in a precise substitution of mutant sequences for wild-type (WT) sequences.

The 3.3-kb *Bam*HI-*Eco*RV and the 2.6-kb *Bam*HI-*Eco*RI fragments of pLF34 were cloned into pBS-KS to yield yAR8left and yAR8right, respectively. These fragments were used to probe fork direction gels.

(ii) *ARS310*. *Bam*HI linkers (NEB) were added to the 850-bp *Eco*RV fragment containing *ARS310* (43), and the fragment was cloned into the *Bam*HI site of pRS326. The *Eco*RV fragment contains nucleotides 166495 to 167340 of the chromosome III sequence. Using this backbone, mutant derivatives were made by the method of Kunkel (36), except for the 106-bp deletion, which was generated by fusion PCR (28). These alterations, indicated by lowercase letters, were introduced in the ACS match B (ATTTACATaaA), match C (TTTTACTTaaT), and match E (ATTTATGagAT). The 2.2-kb *Bam*HI-*Xba*I fragment of plasmid H9G1-1 (43) was cloned into a derivative of pRS306 (54) deleted for sequences between the *Kpn*I and *Sma*I sites of the polylinker to yield ARS310BX. To transfer the mutations into the chromosome, the 500-bp *Spe*I-*Hpa*I fragment from the mutants was ligated to ARS310BX digested with the same enzymes. The resulting plasmids were linearized with *Xho*I to direct integration for two-step gene replacement (6) as was done for *ARS101*.

The 2.9-kb *Pst*I-*Sac*II fragment of K3B (43) was cloned into pRS304 (54) to yield 310left.

Analysis of replication intermediates. Preparation of genomic DNA and two-dimensional gel electrophoresis were performed as described previously (57). For the fork direction analysis of *ARS310*, 60 μg of DNA was digested with *Bam*HI plus *Pst*I. The reaction mix was adjusted to 1 M NaCl and subjected to benzoylated naphthoylated DEAE-cellulose (Sigma Chemical Co., St. Louis, Mo.) chromatography as described by Dijkwel et al. (18), except that all volumes were cut in half.

Images were obtained on a Molecular Dynamics (Sunnyvale, Calif.) PhosphorImager (model PSI or 445SI). Fork direction gels were quantitated by drawing polygons around the arcs and computing volumes using ImageQuant V.5.0.

ORC footprinting. Probes were made by PCR (1) using one primer that had been end labeled using [γ-^{32}P]ATP (New England Nuclear) and polynucleotide kinase (NEB) and one unlabeled primer. For *ARS101*, the labeled primer was positioned 70 bp upstream of the closest match to the ACS, and the unlabeled primer was the T7 reverse primer. For *ARS310*, the end-labeled primer was positioned 95 bp upstream of the closest match to the ACS, and unlabeled M13 reverse primer was used. Footprinting reactions were performed as described by Klemm et al. (34). Recombinant ORC was a generous gift from Stephen Bell (MIT). Chemical sequencing reactions were performed as described by Richterich et al. (51).

Oligonucleotides. All oligonucleotides were synthesized by the Molecular Resources Facility of the New Jersey Medical School. Sequences are available upon request.

RESULTS

***ARS101* contains two redundant matches to the ACS.** A construct designed to replace the *SEN34* open reading frame (ORF) on chromosome I was found to have ARS activity (A. Barton and D. Kabak, personal communication). Subcloning DNA from this region, we identified a 650-bp *Eco*RV-*Cla*I fragment that was Ars$^+$ (Fig. 1A). Two-dimensional (2D) gel analysis revealed that this ARS element was an active origin on chromosome I (Fig. 2A). We designated this ARS element *ARS101*, as it is the first ARS element identified on chromosome I. Analysis of the sequence of the 650-bp *Eco*RV-*Cla*I fragment revealed a single 11 of 11 match to the ACS (ATT TATATTTA). Surprisingly, when we altered this sequence to ATTTATcTagA, the mutant fragment (Xba mutant) was still Ars$^+$, though with reduced activity (Fig. 1B), and still weakly active as an origin in its native chromosomal context (Fig. 2B).

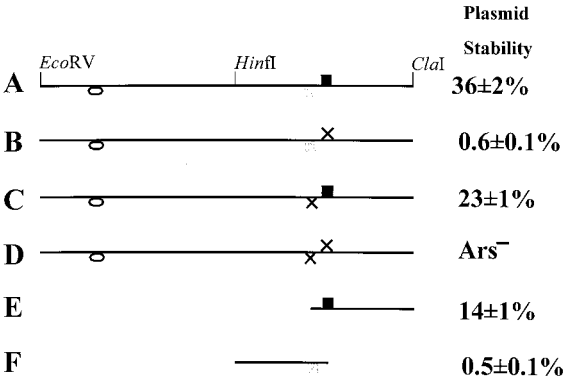

FIG. 1. Two ACS matches in *ARS101*. Line diagrams of *ARS101* and mutant derivatives. The black box indicates the 11 of 11 match to the ACS (strong ORC binding site), and the grey box indicates the 9 of 11 match to the ACS (weak ORC binding site). The oval indicates an additional weak ORC binding site which does not contribute to ARS activity. X's indicate ACS knockout mutations. Plasmid stabilities are expressed as the percentage of plasmid-bearing cells present in a log-phase culture grown under selection. (A) WT 650-bp *Eco*RV-*Cla*I fragment. (B) The 11 of 11 match (Xba) mutant. (C) The 9 of 11 match (Msc) mutant. (D) Double mutant. (E) *Msc*I-*Cla*I subclone, derived from C. (F) *Xba*I-*Hin*FI subclone, derived from B.

One possible explanation for the residual activity of the Xba mutant is that ORC is still able to bind to the mutant sequence, though with lower affinity. We considered this unlikely for two reasons. First, in every previous case where it had been examined, mutation of two of the three highly conserved T's at positions 8, 9, and 10 of the ACS had abolished ARS activity. Second, mutation or modification at these three positions strongly inhibits ORC binding (3, 37, 56). Alternatively, the residual activity might depend on ORC binding to other sequences in the fragment. To rule out ORC binding to the mutant sequence and to identify other ORC binding sites, we performed in vitro ORC footprinting (34) on the WT and mutant fragments. As shown in Fig. 3, ORC bound to and protected a 45-bp region of the WT fragment that includes the 11 of 11 match to the ACS and extends into domain B. However, ORC binding to this site did not induce any hypersensitive sites in the domain B region, as is commonly seen in other ARS elements. In the fragment containing the Xba mutation of the exact match to the ACS, ORC failed to bind the mutant sequence, but rather bound just upstream of the mutant sequence, at a 9 of 11 match to the ACS, inducing three hypersensitive sites not seen in the footprint of the WT fragment (Fig. 3). ORC also bound weakly to a site near the *Eco*RV end of the fragment, which can be seen as partial protection of a region near the top of the gel in Fig. 3. No sequence matching the ACS at nine or more positions was found near this protected region. These observations indicated that ORC does not bind to the mutated sequence and suggested that one or both of the two weak ORC binding sites contributes the weak ARS activity of the mutant fragment.

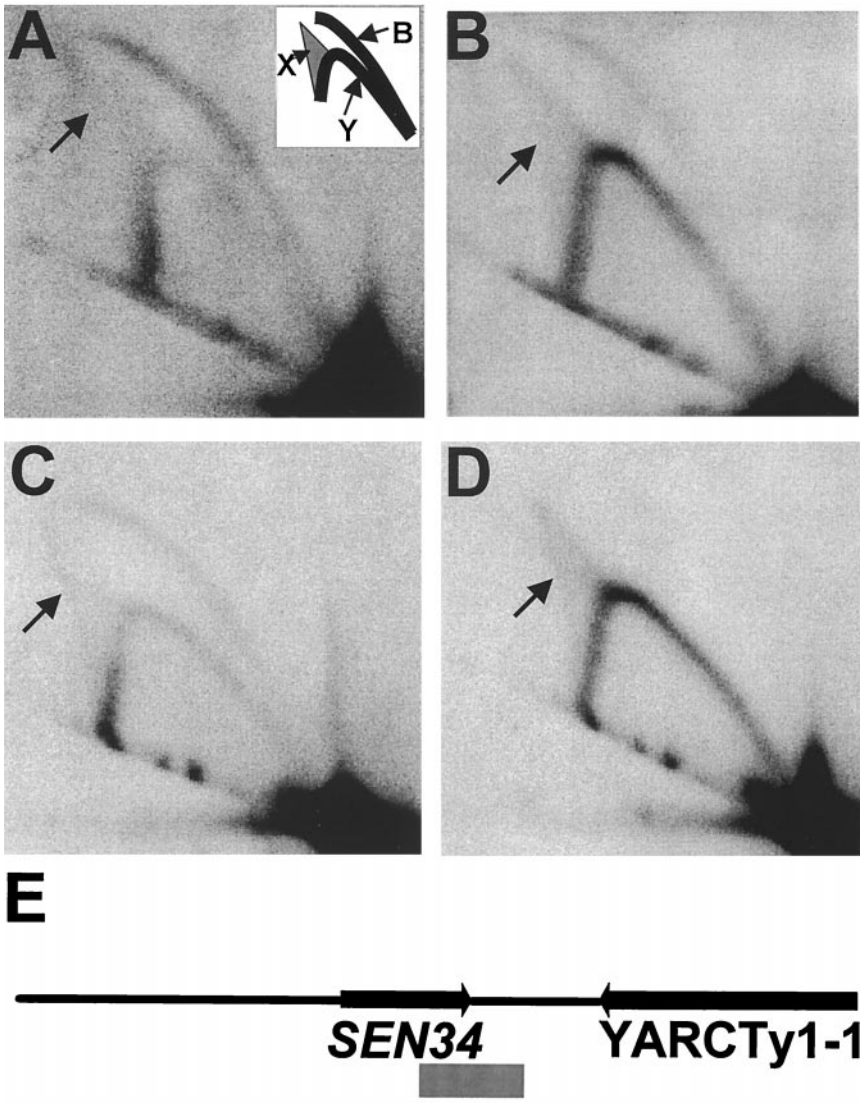

FIG. 2. 2D gel analysis of chromosomal replication origin activity of *ARS101* and mutant derivatives. (A) WT. (B) The 11 of 11 match mutant. (C) The 9 of 11 match mutant. (D) Double mutant. Arrows point to double-Y-shaped replication intermediates, indicative of termination. The inset in panel A is a schematic of replication intermediates as displayed by 2D gel analysis. The arc labeled B corresponds to bubble-shaped molecules, and the one labeled Y corresponds to Y-shaped molecules; the grey triangle labeled X corresponds to the region containing double-Y-shaped (termination) intermediates. (E) Diagram of the 5.3-kb *Eco*RI fragment examined by 2-D analysis. The positions of the *SEN34* ORF and the included part of the adjacent Ty element are shown. The position of the 650-bp *Eco*RV-*Cla*I fragment is indicated by the grey box.

To determine which of these weak ORC binding sites was responsible for ARS activity, the mutant 650-bp *Eco*RV-*Cla*I fragment was digested with *Hin*fI, and the two halves were cloned. Only the 310-bp *Hin*fI-*Cla*I fragment was Ars^+ (data not shown), suggesting that the 9 of 11 match to the ACS (TT**A**TATGT**C**TA, nonconsensus positions in boldface) is responsible for the residual ARS activity in the mutant. To test this hypothesis, we altered this sequence to TT**A**TATGg**C**cA (Msc mutant) in both the WT 650-bp fragment and the Xba mutant fragment. The double mutation abolished ARS activity (Fig. 1D), while the Msc mutation alone had only a modest effect on plasmid stability (Fig. 1C).

To assess the effect of these mutations on origin activity, they were used to replace the WT chromosomal copy of *ARS101*. While the WT origin was quite active, the double mutant was completely inactive, as indicated by the absence of bubble-shaped replication intermediates (compare Fig. 2A with 2D). As expected from their effects on plasmid stability, the mutation in the strong ORC binding site (the Xba mutant) caused a more dramatic reduction in origin activity than the mutation in the weak binding site (the Msc mutant) (compare Fig. 2B to 2C).

Modification of the 2D gel electrophoresis technique to include an in-gel digestion of replication intermediates between running the first and second dimensions allows one to separate the intermediates arising from a replication fork traversing a given fragment in one direction from those arising from a fork traversing the fragment in the opposite direction (22). In an attempt to quantitate the effects of these mutations on chromosomal replication origin activity, fork direction analyses

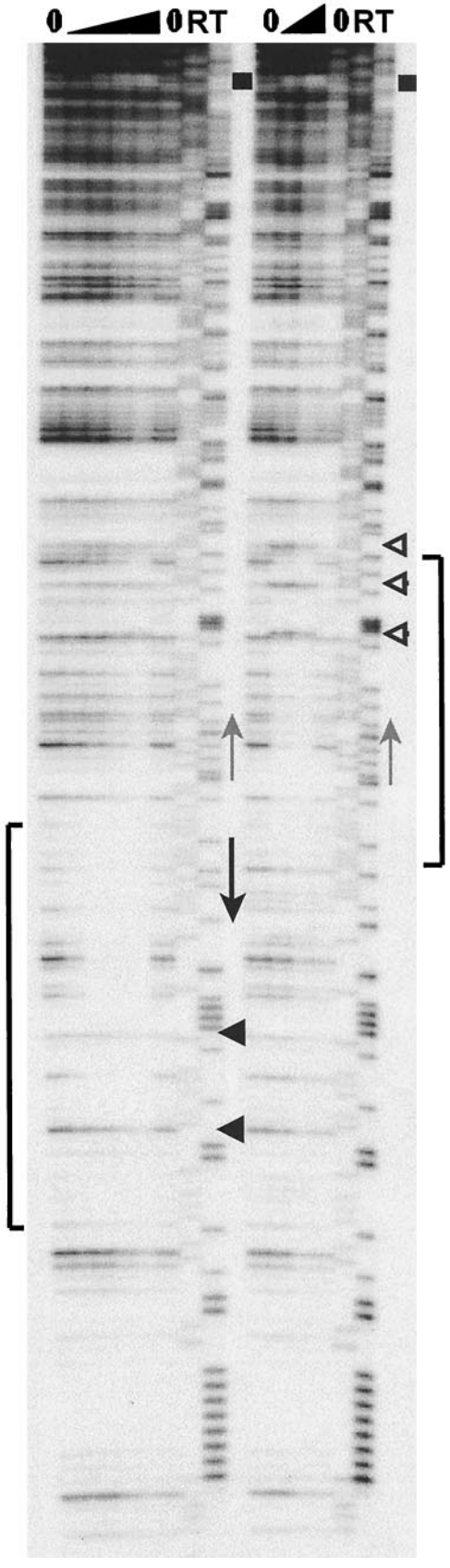

FIG. 3. In vitro ORC footprint of *ARS101*. The left panel shows the footprint of WT *ARS101* labeled near the *Cla*I end (see Fig. 1A). The black arrow marks the position of the 11 of 11 match to the ACS, and the grey arrow marks that of the 9 of 11 match. The region of protection resulting from ORC binding is indicated by the bracket, and the solid black arrowheads mark the positions of two relatively unaffected sites within this region. Lanes labeled 0 contain no ORC protein, and the triangle indicates lanes with increasing amounts of ORC (12.5, 25, 50, and 100 ng for the WT, 100 and 200 ng for the Xba mutant). R and T, A+G and T sequencing lanes, respectively. The black box indicates a weak ORC binding site near the top of the gel. The right panel shows the footprint of the 11 of 11 match mutant. Notice the lack of protection over that match. Protection (region delineated by the bracket) is seen over the 9 of 11 match (grey arrow), and the open arrowheads mark the positions of three hypersensitive sites induced by ORC binding to the 9 of 11 match.

were performed in the regions flanking *ARS101*. In the case of *ARS101*, these analyses were complicated by two factors. First, when *ARS101* was inactivated, forks initiated at flanking origins converged on this region, resulting in a termination zone. The double-Y termination intermediates can be seen in the 2D gel patterns of the mutants (Fig. 2). Second, a Ty1 element lies immediately to the right of *ARS101* (Fig. 4A), necessitating the examination of fragments on the opposite side of this repetitive element. Figure 4 shows the fork direction analysis of the WT and double mutant on both sides of *ARS101*, and the quantitation of these and other results is presented in Table 1. In the patterns obtained from the WT ARS (Fig. 4D and E), the most intense signals are from forks moving away from the ARS, while in the double mutant (Fig. 4F and G) the patterns are reversed, with the most intense signals reflecting forks moving toward the ARS. The best estimate of the activity of WT *ARS101* is provided by the analysis of the left side, because the fragment analyzed is directly adjacent to the ARS element. In this case, about 90% of the forks are coming from *ARS101* in the WT, while only 20% are moving in the same direction in the double mutant, which is inactive, as judged from 2D gels. If the 20% signal seen in the double mutant contributes to the signal seen in the WT, it would suggest that *ARS101* is active only about 70% of the time. The results of the analysis of the right side are consistent with this conclusion, with about two-thirds of the forks moving away from the ARS in the WT and only 8% of the forks moving away from the ARS in the mutant. Mutation of the 11 of 11 match to the ACS reduced chromosomal origin activity of *ARS101* to about half of the WT level, while mutation of the 9 of 11 match had no significant effect on chromosomal origin activity in this analysis (Table 1).

Inactivation of *ARS310* requires mutation of three ACS matches. We also examined *ARS310* as part of our analysis of replication origins on chromosome III (15, 19, 42, 56, 57). *ARS310* was localized to an 850-bp *Eco*RV fragment (43, 48). This fragment contains one 11 of 11 match to the ACS (match B, ATTTACATTTA) and three 10 of 11 matches (A, C, and E). Each match was mutated independently in a plasmid carrying the 850-bp fragment, and none of these mutations abolished ARS activity, though mutation of one of the 10 of 11 matches (match C, TTTTAC**T**TTTT) dramatically reduced activity (Fig. 5 and data not shown). The match C mutation was paired with mutations in each of the other matches. One pair (B^-C^-, Fig. 5F) abolished ARS activity while the remaining

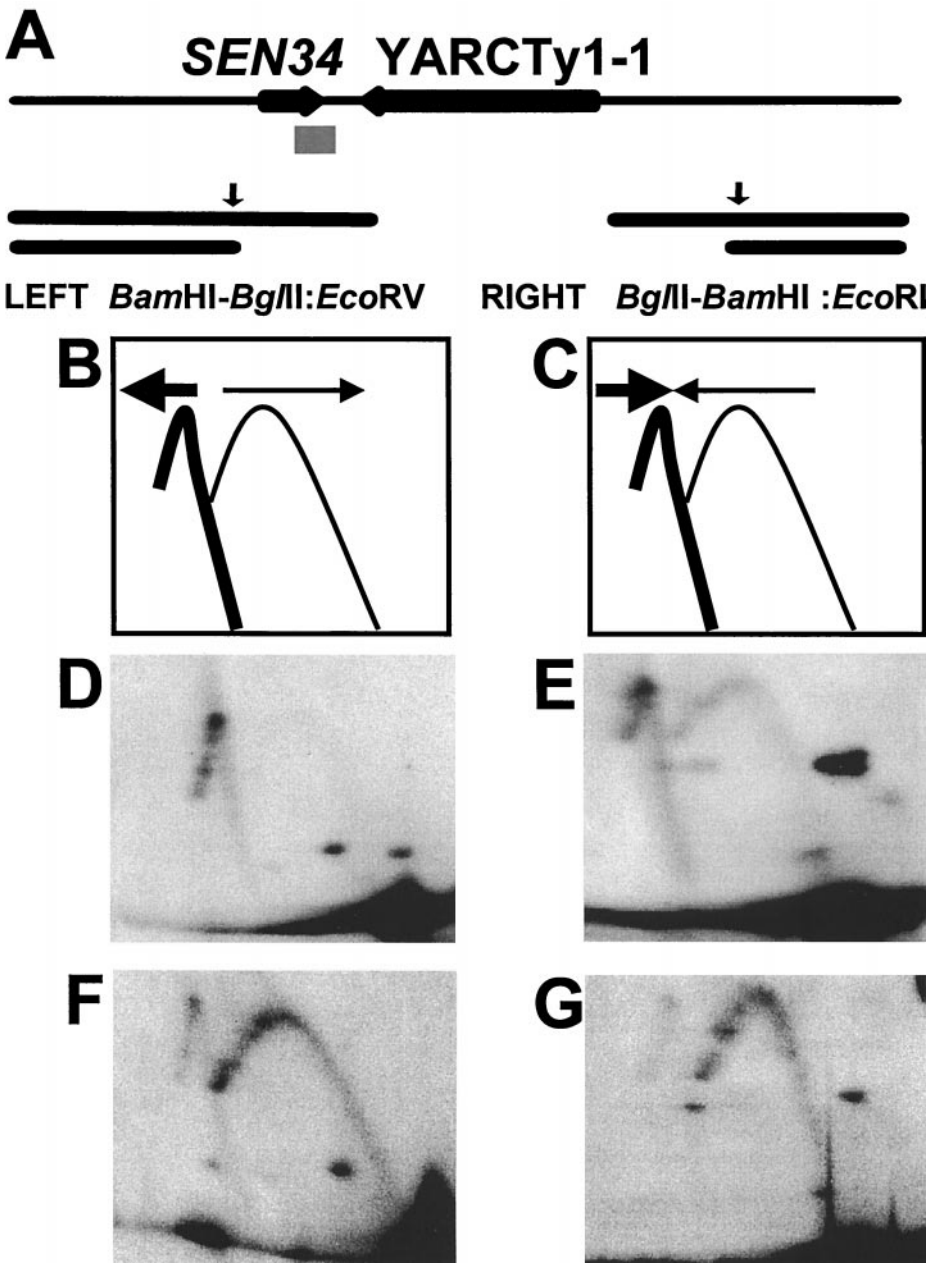

FIG. 4. Fork direction analyses flanking *ARS101*. (A) The upper line depicts the 13.9-kb *Bam*HI fragment containing *ARS101*. The positions of the *SEN34* ORF and YARCTy1-1 are indicated by arrows. The position of the 650-bp *Eco*RV-*Cla*I fragment containing *ARS101* is shown by the grey box below the line. Below this are the 5.6-kb *Bam*HI-*Bgl*II fragment, used to examine fork direction to the left of *ARS101*, and the 4.5-kb *Bgl*II-*Bam*HI fragment, used on the right. The arrows mark the positions of the *Eco*RV and *Eco*RI sites used for in-gel digestion prior to the second dimension. The probes used are indicated below these lines. As discussed by Friedman and Brewer (22), in-gel digestion allows one to distinguish rightward-moving replication forks from leftward-moving ones. How these replication intermediates are resolved depends on the geometry of the origin, the site of digestion, and the probe used to detect them. (B) Schematic diagram for fork direction analysis to the left of *ARS101*. Replication intermediates from leftward-moving (thick arrow) forks, including those emanating from *ARS101*, are shown as a thick line. Intermediates from rightward-moving (thin arrow) forks, i.e., those moving towards *ARS101* are shown as a thin line. (C) Schematic diagram for fork direction analysis to the right of *ARS101*. Replication intermediates from rightward-moving (thick arrow) forks, including those emanating from *ARS101*, are shown as a thick line. Intermediates from leftward-moving (thin arrow) forks, those moving towards *ARS101*, are shown as a thin line. (D) Left side, WT. (E) Right side, WT. (F) Left side, double mutant. (G) Right side, double mutant.

double mutant pairs had activities similar to that of the match C mutant alone (data not shown).

To examine the effect of the B^-C^- double mutation on origin activity, a two-step gene replacement strategy was used. Two surprising results were obtained. The replacement construct, which carried the double mutation on a 2.2-kb *Bam*HI-*Xba*I fragment (Fig. 5A), was weakly Ars^+ (data not shown), and the doubly mutant chromosomal origin was also weakly active, as evidenced by the presence of bubble-shaped intermediates on 2D gels (Fig. 6E). We also noted the presence of

TABLE 1. Quantitation of fork direction analyses of *ARS101*

ARS101 derivative	Mean % of forks[a] ± SD	
	Left of *ARS101*	Right of *ARS101*
WT	87 ± 1	66 ± 4
11 of 11 match mutant	48 ± 1	17 ± 8
9 of 11 match mutant	95 ± 4	75 ± 7
Double mutant	20 ± 1	8 ± 2

[a] Results are expressed as the percentage of forks coming from the direction of *ARS101*, i.e. from the right on the left side and from the left on the right side.

a replication fork pause site, indicated by intense spots on the Y arcs in Fig. 6E and F (arrows) that reflect accumulation of large Y-shaped replication intermediates. Replication forks pause when they encounter a tRNA gene whose direction of transcription opposes the direction of movement of the replication fork (16). The direction in which forks traverse this fragment when *ARS310* is not active (see below) and the position and orientation of a glutamine tRNA gene (Fig. 6A) are consistent with the observed pause site.

The WT, B^-, C^-, and B^-C^- *Bam*HI-*Xba*I fragments were transferred to a *CEN* vector, and ARS activity was quantitated. As indicated in Fig. 5B, plasmids carrying the WT *ARS310* in the *Bam*HI-*Xba*I fragment are considerably more stable than plasmids carrying the 850-bp *Eco*RV fragment. Since ARS activity was detected only in the 850-bp *Eco*RV fragment and not in flanking fragments (43), sequences present in the larger context must stimulate the activity of the minimal *ARS310* fragment. Experiments are under way to characterize these stimulatory sequences (data not shown). These stimulatory sequences also act on the B^-, C^-, and B^-C^- mutants. The B^- mutant shows approximately the same plasmid stability as the WT in both fragment contexts (Fig. 5C), while the C^- mutant shows reduced plasmid stability in both contexts (Fig. 5D). While the B^-C^- double mutant appears to be Ars^- in the 850-bp *Eco*RV fragment, extremely weak ARS activity is detected in the context of the *Bam*HI-*Xba*I fragment (Fig. 5F). Presumably, in the absence of these stimulatory sequences, the ARS activity of the double mutant is reduced to the point where the primary transformants fail to give rise to colonies when streaked on selective plates. Hence, the double mutant appears to be Ars^- in the context of the 850-bp *Eco*RV fragment.

As in the case of *ARS101*, ORC footprinting was used to identify the sequences responsible for the residual activity of the B^-C^- mutant. In the WT fragment, ORC footprinted over the B and C matches, apparently binding with similar affinity at both sites (Fig. 7). Binding at both sites resulted in the induction of hypersensitive sites in similar positions relative to the ACS matches as seen in other ARS elements. The B and C matches to the ACS are separated by only 45 bp, yet ORC was able to bind at both sites simultaneously. Binding to these sites did not appear to be cooperative, since ORC bound to match B in the C^- mutant and to match C in the B^- mutant with affinities similar to those seen with the WT fragment.

In the B^-C^- fragment, as expected, ORC failed to bind to the mutant matches. Instead, binding was detected over another 10 of 11 match to the ACS (match E, ATTTATGTTAT), which is separated from match C by 26 bp (Fig. 7). This difference is most clearly seen in the region of the footprint delineated by the uppermost brackets. In the WT and B^- fragments, a pair of strong hypersensitive sites was induced at the bottom of this region and a weak pair of hypersensitive sites was induced at the top. The region between these pairs of hypersensitive sites was strongly protected. In the C^- and B^-C^- fragments, only the lower site of the pair of hypersensitive sites at the bottom of the region was induced. In these mutants, the hypersensitive sites at the top of the region were missing, as was the region of strong protection seen in the WT fragment. Instead, all the DNase I cleavage sites in this region decreased to the same extent. To confirm that the binding detected in the B^-C^- mutant is due to match E, the sequence was altered to create the $B^-C^-E^-$ mutant. As shown in Fig. 7, ORC fails to bind to any of the mutated sites in this fragment.

The in vitro footprinting data suggested that the residual ARS and origin activity of the B^-C^- mutant was due to ORC recognition of match E. To confirm this hypothesis, the triple mutant was tested for ARS activity in the context of the 2.2-kb *Bam*HI-*Xba*I fragment and found to be Ars^- (Fig. 5G). Similarly, replacing the WT ARS in the chromosome with the $B^-C^-E^-$ mutant abolished origin activity (Fig. 6F). Thus, inactivation of *ARS310* required mutation of three matches to the ACS within a 104-bp region. Despite being unaltered in the $B^-C^-E^-$ mutant, the remaining 10 of 11 match (match A, TTTCATGTTTA) apparently does not contribute to either ARS or chromosomal replication origin function.

To quantitate the effects of these mutations on origin activity, fork direction analyses were performed. No effects of these mutations were seen in the region to the right of *ARS310*, which was replicated by forks moving rightward through the

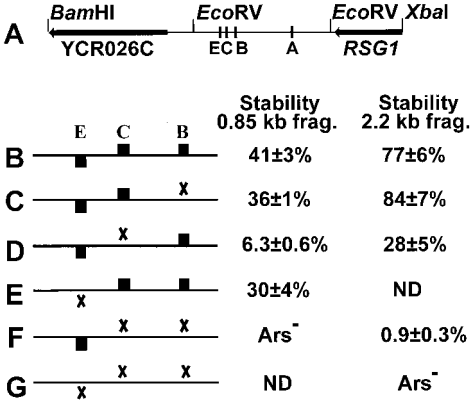

FIG. 5. Three ACS matches contribute to *ARS310* activity. (A) Diagram of the 2.2-kb *Bam*HI-*Xba*I fragment containing *ARS310*. Arrows indicate the included portions of the YCR026C and *RSG1* ORFs. The positions of ACS matches E, C, B, and A are marked by lines. The *Eco*RV sites defining the 0.85-kb fragment are indicated. (B to G) Plasmid constructs carrying the WT *ARS310* and various ACS mutant derivatives. Black boxes represent the ACS matches, while X's denote knockout mutations; match A is not contained in the region shown and is unaltered in all the constructs. ND, not determined. Plasmid stabilities are reported for two contexts, the 0.85-kb *Eco*RV fragment (frag.) and the 2.2-kb *Bam*HI-*Xba*I fragment. The larger fragment contains a stimulator of ARS activity, as indicated by the increased stabilities of all the constructs in the *Bam*HI-*Xba*I context. While the B^-C^- double knockout appears to be Ars^- in the context of the *Eco*RV fragment, it is weakly active in the larger context (F). The triple mutant is Ars^- in this context (G).

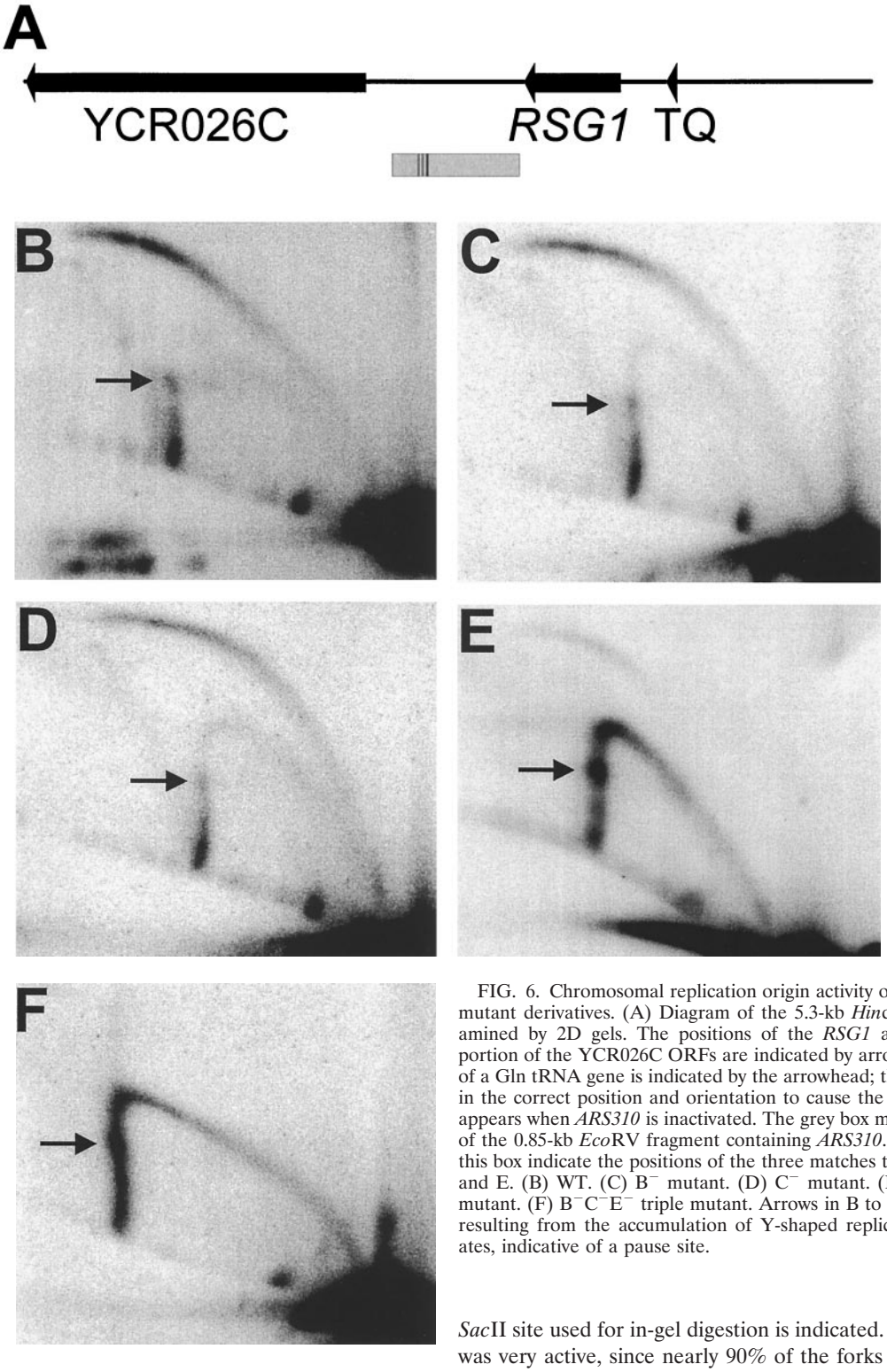

FIG. 6. Chromosomal replication origin activity of *ARS310* and its mutant derivatives. (A) Diagram of the 5.3-kb *Hin*dIII fragment examined by 2D gels. The positions of the *RSG1* and the included portion of the YCR026C ORFs are indicated by arrows. The position of a Gln tRNA gene is indicated by the arrowhead; this tRNA gene is in the correct position and orientation to cause the pause site which appears when *ARS310* is inactivated. The grey box marks the position of the 0.85-kb *Eco*RV fragment containing *ARS310*. The lines within this box indicate the positions of the three matches to the ACS, B, C, and E. (B) WT. (C) B^- mutant. (D) C^- mutant. (E) B^-C^- double mutant. (F) $B^-C^-E^-$ triple mutant. Arrows in B to F point to a spot resulting from the accumulation of Y-shaped replication intermediates, indicative of a pause site.

fragment (data not shown). The analysis of the region to the left of *ARS310* is presented in Fig. 8 and Table 2. Figure 8A is a diagram of the 4.8-kb *Pst*I-*Bam*HI fragment used for this analysis. The *Bam*HI site defining the right end of this fragment is the same as the site defining the left end of the 2.2-kb *Bam*HI-*Xba*I fragment shown in Fig. 5A. The position of the *Sac*II site used for in-gel digestion is indicated. The WT origin was very active, since nearly 90% of the forks came from the direction of *ARS310*, to the right of the fragment analyzed (Fig. 8C and Table 2). The mutations in matches B and C had little effect individually, but the B^-C^- double mutation dramatically reduced origin activity (Fig. 8D and Table 2). In the $B^-C^-E^-$ mutant, the fraction of forks coming from the right was even further reduced, to about 10% (Fig. 8E and Table 2). We conclude that the triple mutation completely inactivates the

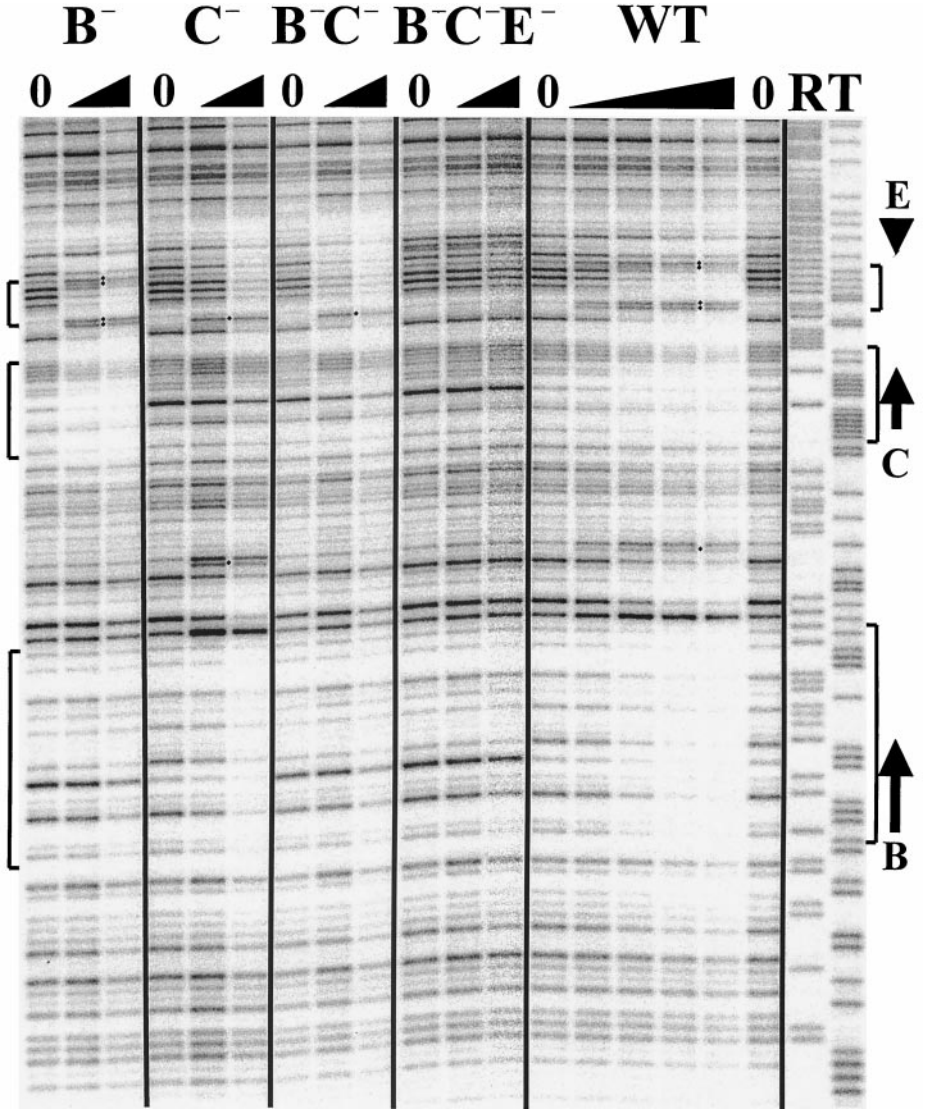

FIG. 7. In vitro ORC footprint of *ARS310*. The footprints of WT *ARS310* and four mutant derivatives, single knockouts of ACS matches B and C, the B^-C^- double mutant, and the $B^-C^-E^-$ triple knockout mutant, are shown. The positions of ACS matches B, C, and E are marked by the arrows on the right side. The uppermost brackets mark the region where ORC binding to match C versus match E is readily distinguished. The middle and lower brackets mark the regions protected by ORC binding to matches C and B, respectively. Hypersensitive sites are marked by dots. Labels on individual lanes are as in Fig. 3. The amounts of ORC used for the WT fragment were 10, 20, 40, and 60 ng, and for the mutant fragments they were 20 and 60 ng.

chromosomal origin, based on the observation that similar frequencies of forks moving leftward through the fragment analyzed are detected in the 106-bp deletion mutant, in which all three matches were removed, and the triple mutant (Table 2).

DISCUSSION

We have described our characterization of two ARS elements, *ARS101* and *ARS310*, both of which are active as origins in their native locations. These ARS elements differ from those described previously in that multiple matches to the ACS must be altered to inactivate ARS and origin function. In previous analyses, alteration of a single match to the ACS was sufficient to abolish ARS function (7, 47, 56, 57, 61, 62). Despite the fact that *ARS1* contains multiple weak ORC binding sites (3), mutations in the exact match to the ACS, the preferred ORC binding site, abolish ARS activity (40). In contrast, in the case of *ARS101*, two matches to the ACS, separated by 8 bp, must be altered to eliminate ARS and origin activity. These two matches appear to represent independent ARS elements, as

TABLE 2. Fork direction analyses to the left of *ARS310*

ARS310 derivative	Mean % of forks[a] ± SD
WT	88 ± 1
B^- mutant	83 ± 1
C^- mutant	78 ± 4
B^-C^- double mutant	24 ± 5
$B^-C^-E^-$ triple mutant	10 ± 4
Deletion mutant	15

[a] Coming from the right, the direction of *ARS310*.

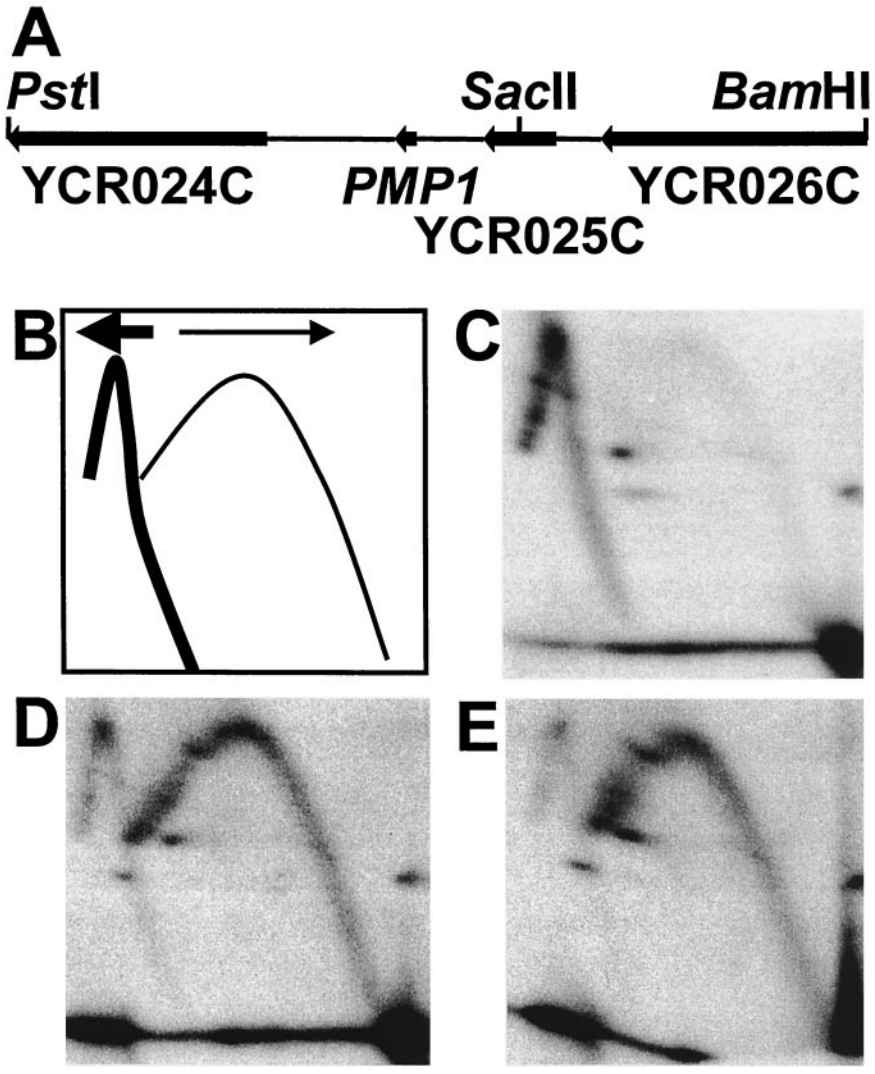

FIG. 8. Fork direction analysis to the left of *ARS310*. (A) The 4.8-kb *Pst*I-*Bam*HI fragment examined in this analysis is shown. It is directly adjacent to the left end of the 2.2-kb *Bam*HI-*Xba*I fragment shown in Fig. 5A. The positions of the YCR025C and *PMP1* ORFs and the included portions of the YCR024C and YCR026C ORFs are shown. The *Sac*II site used for in-gel digestion is also indicated. The 2.9-kb *Pst*I-*Sac*II fragment was used as a probe. (B) Schematic diagram for fork direction analysis to the left of *ARS310*. Replication intermediates arising from leftward-moving (thick arrow) forks, including those emanating from *ARS310*, are shown as a thick line. Intermediates from rightward-moving (thin arrow) forks, those moving towards *ARS310*, are shown as a thin line. (C) WT. (D) B^-C^- double mutant. (E) $B^-C^-E^-$ triple mutant.

they can be cloned separately (Fig. 1). They do not contribute equally to activity, however. As one might expect, the 11 of 11 match to ACS is the preferred ORC binding site in vitro (Fig. 3), and alteration of this site has much more dramatic effects on both ARS (Fig. 1) and origin (Fig. 2) function. The contribution of the 9 of 11 match to the ACS in the WT ARS is unclear. While the 9 of 11 match mutation gave slightly reduced ARS activity, as measured by plasmid stability (Fig. 1), it had no significant effect on origin activity, as measured by 2D gel (Fig. 2) and fork direction (Table 1) analyses.

The analysis of *ARS310* revealed that three matches to the ACS, one 11 of 11 match and two 10 of 11 matches, within a 104-bp region must be altered to inactivate both ARS and origin activity. Somewhat surprisingly, the 11 of 11 match does not seem to be the major contributor to activity. While the mutation of match B, the 11 of 11 match, caused little or no reduction in ARS activity, it was the mutation of match C which dramatically reduced activity (Fig. 5). However, this apparent dominance of match C was not mimicked by ORC binding, since ORC footprinted equally well over matches B and C in vitro (Fig. 7), nor by the effects of these mutations on origin activity, since the B^- and C^- mutants had similar small reductions in activity (Fig. 6 and Table 2). At this point, we do not understand the basis of the differential effects of the C^- mutation in the plasmid and chromosomal contexts.

While these analyses do not allow us to assess the contributions of the individual ACS matches to origin function, it should be possible to do so utilizing the replication initiation point (RIP) mapping technique of Gerbi and Bielinsky (24). The chromosomal copy of *ARS1* shows a single initiation point located 30 bp from the ACS (4). Assuming that each match to the ACS of *ARS310* specifies its own start site, it should be

TABLE 3. Compound origins in *S. cerevisiae*

ARS	No. of matches	Spacing (bp)
ARS101	2	8
ARS310	3	82
ARS603	2	5
ARS601/602	2	241
ARS302/303/320	3	580
HMRE	≥3	≤865

possible to determine the frequency of initiation for each match in the WT origin by RIP mapping. Applying this technique to mutant *ARS310* derivatives would also reveal whether each match uses its own start site or if they all use a common one.

The compound nature of *ARS310* is not conserved in a closely related *Saccharomyces* species. We have analyzed several ARS elements from the homeologous chromosome III present in the brewing strain *Saccharomyces carlsbergensis* (58, 65). *ARS310*^{carl} has a single essential match to the ACS which is in a short region of homology (18 of 21 bp) that includes match E in *S. cerevisiae ARS310*. Matches B and C are not conserved in *ARS310*^{carl}. In *S. cerevisiae*, match E has a T-to-A transversion at position 10 of the ACS relative to its *S. carlsbergensis* counterpart. This change in the ACS is known to inactivate *ARS307* (59), and the modification of position 10 strongly inhibits ORC binding at *ARS1* (37). Therefore, it is not surprising that ORC has a lower affinity for match E than it does for matches B and C.

Having found these two unusual replication origins, we wondered how frequent such origins might be in the genome. We adopted a simple definition for a compound origin: functionally redundant ACS matches within the same intergenic region. For practical reasons, we used inter-ORF regions in our analysis. We realize that this is not a perfect definition. For example, the essential matches to the ACS for *ARS604* and *ARS605* reside within the *BLM3* and *MSH4* ORFs, respectively. In addition, the B3 element of *ARS1* lies within the *TRP1* ORF. Therefore, sequences important for origin function can reside within an ORF. However, single, essential matches to the ACS have been defined for 22 ARS elements, and 20 of these fall within intergenic regions. The inactivation of *ARS603* required the mutation of two closely spaced matches, both of which lie in an intergenic region. An analysis of these 23 ARS elements revealed four additional compound origins (Table 3). We suggest that, like the two fragments of *ARS101*, *ARS601* and *ARS602* should be considered a single compound element, as should *ARS302*, *ARS303*, and *ARS320*. These five ARS elements were given individual ARS designations because nonoverlapping subclones were shown to have ARS activity (43, 53, 61). However, given the close proximity of the essential ACSs (250 bp for *ARS601/602* and approximately 600 bp for *ARS302/303/320*), it is unlikely that these clusters of ARS elements function independently. In fact, it has been reported that, both on plasmids and in the chromosome, ARS elements separated by as much as 6 kb interfere with each other, so that only one of the two ARS elements fires in any replication cycle (8, 9, 39). The sequences responsible for the activity of the *HMRE* ARS are less well defined than the others, but Hurst and Rivier (31) reported that three separate fragments, spanning 865 bp, have ARS activity, while Palacios DeBeer and Fox (45) extended this observation by demonstrating chromosomal replication origin activity for three fragments in *HMRE*.

In *ARS603*, the ACS matches are oriented so that each match lies within the first 16 bp of domain B of the other match, making it unlikely that nonoverlapping subclones with ARS activity could be found (53). *ARS310* presents a somewhat similar situation. Matches C and E are in opposite orientations, separated by 26 bp. Therefore, this 26-bp interval is shared by the domain B regions of both matches. Matches B and C are in the same orientation, with match B only 45 bp upstream of match C. While the individual functional elements have not been defined experimentally, the domain B regions for the different ACS matches of *ARS310* clearly overlap.

In summary, 6 of the 22 ARS elements examined are compound elements. This would suggest that one-quarter to one-third of the origins in the *S. cerevisiae* genome are compound origins. Could this frequency of compound origins arise by chance? We have analyzed the complete sequences of three regions of the yeast genome in which ARS elements have been identified systematically, chromosomes III and VI and a 131-kb region of chromosome XIV (23). This 716 kb represents about 6% of the genome. There are 33 ARS elements, of which 27 are detectably active as chromosomal replication origins, in these three regions, which also contains 359 inter-ORF regions (23, 42, 53, 64). Since less than 8% of the inter-ORF regions contain origins, the frequency of compound origins is much higher than expected. The origin-containing regions are distinguished from their counterparts neither by their size nor by the orientations of their flanking ORFs (C. S. Newlon, unpublished data).

While *S. cerevisiae* has proven to be an excellent model for many aspects of mammalian DNA replication, *S. cerevisiae* DNA replication origin structure has appeared to be different from that of other eukaryotes. *ARS1*, the paradigm *S. cerevisiae* origin, is small, about 120 bp (40), and has a single binding site for ORC, which contains the essential match to the ACS (3). In addition, replication initiates at a discrete site, as determined both by 2D gels (10) and RIP mapping (4, 5). In contrast to the highly specific replication initiation sites typical of *S. cerevisiae*, replication initiation events in mammalian cells appear to be distributed through large "initiation zones" (reviewed by DePamphilis [14]). The extreme case (out of more than 10 mammalian replication origins analyzed) is the well-studied dihydrofolate reductase (DHFR) replication origin of Chinese hamster ovary cells, in which 2D gel analyses detect bubble shaped-replication intermediates throughout a 55-kb region (17, 60). Other approaches to mapping replication initiation sites, e.g., detection of the earliest-labeled fragments, nascent-strand abundance assays, and fork polarity assays, often reveal preferred initiation sites within these initiation zones. In the DHFR origin, these approaches have identified three preferred sites, oriβ, oriβ′, and oriγ (11, 26, 27, 35). While the detection of preferred initiation sites suggests the presence of multiple functional elements within initiation zones, it is also possible that a single element specifies initiation events anywhere within a broad region. Support for the presence of such an element in the DHFR origin has been provided recently by the finding that a 3.2-kb fragment at one end of the initiation zone appears to be required for all initiation activity within the

zone (32). The presence of multiple elements would clearly be analogous to the compound origins of *S. cerevisiae*, which are composed of multiple binding sites for the replication initiator protein ORC.

The analysis of *S. pombe* replication origins has provided clear examples of origins containing multiple functional elements. Individual *S. pombe* ARS elements are larger than their *S. cerevisiae* counterparts, 0.5 to 1.5 kb, and are themselves composed of multiple redundant elements. Detailed dissections have been performed on four ARS elements, *ars1* (13), *ars3001* (33), *ars3002* (20), and *ars2004* (44), and a feature common to all of them is the presence of redundant elements important for ARS function. It is not yet clear if this functional redundancy is analogous to that seen in the *S. cerevisiae* compound origins, i.e., multiple, redundant binding sites for ORC. However, two observations are particularly intriguing in this regard. First, these redundant elements are A+T rich, with a biased strand distribution, i.e., with one strand containing predominantly A and the other strand predominantly T, a pattern reminiscent of the biased strand distribution of A's and T's in the *S. cerevisiae* ACS. Second, Orp4p, a component of the *S. pombe* ORC homolog, binds DNA via AT hooks, a motif that recognizes A+T tracts (12), suggesting that the redundant elements might be binding sites for the replication initiator protein. On a larger scale, *S. pombe* also provides a precedent for the presence of multiple, separable ARS elements within a single replication origin. The *ura4* origin consists of a cluster of three ARS elements, *ars3002*, *ars3003*, and *ars3004*, within a 5.5-kb region (21).

ACKNOWLEDGMENTS

We thank Stephen Bell for the gift of purified ORC and members of the Newlon lab for helpful discussions.

This work was supported by NIH grant GM35678 to C.S.N.

REFERENCES

1. **Ausubel, F. M., R. Brent, R. E. Kingston, D. D. Moore, J. G. Seidman, J. A. Smith, and K. Struhl (ed.).** 1994. Current protocols in molecular biology. John Wiley & Sons, Inc., New York, N.Y.
2. **Becker, D. M., and L. Guarente.** 1991. High-efficiency transformation of yeast by electroporation. Methods Enzymol. **194:**182–187.
3. **Bell, S. P., and B. Stillman.** 1992. ATP-dependent recognition of eukaryotic origins of DNA replication by a multiprotein complex. Nature **357:**128–134.
4. **Bielinsky, A. K., and S. A. Gerbi.** 1999. Chromosomal *ARS1* has a single leading strand start site. Mol. Cell **3:**477–486.
5. **Bielinsky, A. K., and S. A. Gerbi.** 1998. Discrete start sites for DNA synthesis in the yeast ARS1 origin. Science **279:**95–98.
6. **Boeke, J. D., J. Trueheart, G. Natsoulis, and G. R. Fink.** 1987. 5-Fluoroorotic acid as a selective agent in yeast molecular genetics. Methods Enzymol. **154:**164–175.
7. **Bouton, A. H., and M. M. Smith.** 1986. Fine-structure analysis of the DNA sequence requirements for autonomous replication of *Saccharomyces cerevisiae* plasmids. Mol. Cell. Biol. **6:**2354–2363.
8. **Brewer, B. J., and W. L. Fangman.** 1993. Initiation at closely spaced replication origins in a yeast chromosome. Science **262:**1728–1731.
9. **Brewer, B. J., and W. L. Fangman.** 1994. Initiation preference at a yeast origin of replication. Proc. Natl. Acad. Sci. USA **91:**3418–3422.
10. **Brewer, B. J., and W. L. Fangman.** 1987. The localization of replication origins on ARS plasmids in *S. cerevisiae*. Cell **51:**463–471.
11. **Burhans, W. C., L. T. Vassilev, M. S. Caddle, N. H. Heintz, and M. L. DePamphilis.** 1990. Identification of an origin of bidirectional DNA replication in mammalian chromosomes. Cell **62:**955–965.
12. **Chuang, R. Y., and T. J. Kelly.** 1999. The fission yeast homologue of Orc4p binds to replication origin DNA via multiple AT-hooks. Proc. Natl. Acad. Sci. USA **96:**2656–2661.
13. **Clyne, R. K., and T. J. Kelly.** 1995. Genetic analysis of an ARS element from the fission yeast *Schizosaccharomyces pombe*. EMBO J. **14:**6348–6357.
14. **DePamphilis, M. L.** 1999. Replication origins in metazoan chromosomes: fact or fiction? Bioessays **21:**5–16.
15. **Dershowitz, A., and C. S. Newlon.** 1993. The effect on chromosome stability of deleting replication origins. Mol. Cell. Biol. **13:**391–398.
16. **Deshpande, A. M., and C. S. Newlon.** 1996. DNA replication fork pause sites dependent on transcription. Science **272:**1030–1033.
17. **Dijkwel, P. A., and J. L. Hamlin.** 1995. The Chinese hamster dihydrofolate reductase origin consists of multiple potential nascent-strand start sites. Mol. Cell. Biol. **15:**3023–3031.
18. **Dijkwel, P. A., J. P. Vaughn, and J. L. Hamlin.** 1991. Mapping of replication initiation sites in mammalian genomes by two-dimensional gel analysis: stabilization and enrichment of replication intermediates by isolation on the nuclear matrix. Mol. Cell. Biol. **11:**3850–3859.
19. **Dubey, D. D., L. R. Davis, S. A. Greenfeder, L. Y. Ong, J. G. Zhu, J. R. Broach, C. S. Newlon, and J. A. Huberman.** 1991. Evidence suggesting that the ARS elements associated with silencers of the yeast mating-type locus *HML* do not function as chromosomal DNA replication origins. Mol. Cell. Biol. **11:**5346–5355.
20. **Dubey, D. D., S. M. Kim, I. T. Todorov, and J. A. Huberman.** 1996. Large, complex modular structure of a fission yeast DNA replication origin. Curr. Biol. **6:**467–473.
21. **Dubey, D. D., J. Zhu, D. L. Carlson, K. Sharma, and J. A. Huberman.** 1994. Three ARS elements contribute to the *ura4* replication origin region in the fission yeast, *Schizosaccharomyces pombe*. EMBO J. **13:**3638–3647.
22. **Friedman, K. L., and B. J. Brewer.** 1995. Analysis of replication intermediates by two-dimensional agarose gel electrophoresis. Methods Enzymol. **262:**613–627.
23. **Friedman, K. L., B. J. Brewer, and W. L. Fangman.** 1997. Replication profile of *Saccharomyces cerevisiae* chromosome VI. Genes Cells **2:**667–678.
24. **Gerbi, S. A., and A. K. Bielinsky.** 1997. Replication initiation point mapping. Methods **13:**271–280.
25. **Gilbert, D. M.** 1998. Replication origins in yeast versus metazoa: separation of the haves and the have nots. Curr. Opin. Genet. Dev. **8:**194–199.
26. **Handeli, S., A. Klar, M. Meuth, and H. Cedar.** 1989. Mapping replication units in animal cells. Cell **57:**909–920.
27. **Heintz, N. H., and J. L. Hamlin.** 1982. An amplified chromosomal sequence that includes the gene for dihydrofolate reductase initiates replication within specific restriction fragments. Proc. Natl. Acad. Sci. USA **79:**4083–4087.
28. **Ho, S. N., H. D. Hunt, R. M. Horton, J. K. Pullen, and L. R. Pease.** 1989. Site-directed mutagenesis by overlap extension using the polymerase chain reaction. Gene **77:**51–59.
29. **Hsiao, C. L., and J. Carbon.** 1979. High-frequency transformation of yeast by plasmids containing the cloned yeast *ARG4* gene. Proc. Natl. Acad. Sci. USA **76:**3829–3833.
30. **Huang, R. Y., and D. Kowalski.** 1996. Multiple DNA elements in *ARS305* determine replication origin activity in a yeast chromosome. Nucleic Acids Res. **24:**816–823.
31. **Hurst, S. T., and D. H. Rivier.** 1999. Identification of a compound origin of replication at the *HMR-E* locus in *Saccharomyces cerevisiae*. J. Biol. Chem. **274:**4155–4159.
32. **Kalejta, R. F., X. Li, L. D. Mesner, P. A. Dijkwel, H. B. Lin, and J. L. Hamlin.** 1998. Distal sequences, but not ori-beta/OBR-1, are essential for initiation of DNA replication in the Chinese hamster DHFR origin. Mol. Cell **2:**797–806.
33. **Kim, S. M., and J. A. Huberman.** 1998. Multiple orientation-dependent, synergistically interacting, similar domains in the ribosomal DNA replication origin of the fission yeast *Schizosaccharomyces pombe*. Mol. Cell. Biol. **18:**7294–7303.
34. **Klemm, R. D., R. J. Austin, and S. P. Bell.** 1997. Coordinate binding of ATP and origin DNA regulates the ATPase activity of the origin recognition complex. Cell **88:**493–502.
35. **Kobayashi, T., T. Rein, and M. L. DePamphilis.** 1998. Identification of primary initiation sites for DNA replication in the hamster dihydrofolate reductase gene initiation zone. Mol. Cell. Biol. **18:**3266–3277.
36. **Kunkel, T. A., K. Bebenek, and J. McClary.** 1991. Efficient site-directed mutagenesis using uracil-containing DNA. Methods Enzymol. **204:**125–139.
37. **Lee, D. G., and S. P. Bell.** 1997. Architecture of the yeast origin recognition complex bound to origins of DNA replication. Mol. Cell. Biol. **17:**7159–7168.
38. **Lin, S., and D. Kowalski.** 1997. Functional equivalency and diversity of *cis*-acting elements among yeast replication origins. Mol. Cell. Biol. **17:**5473–5484.
39. **Marahrens, Y., and B. Stillman.** 1994. Replicator dominance in a eukaryotic chromosome. EMBO J. **13:**3395–3400.
40. **Marahrens, Y., and B. Stillman.** 1992. A yeast chromosomal origin of DNA replication defined by multiple functional elements. Science **255:**817–823.
41. **Matsumoto, K., and Y. Ishimi.** 1994. Single-stranded-DNA-binding protein-dependent DNA unwinding of the yeast *ARS1* region. Mol. Cell. Biol. **14:**4624–4632.
42. **Newlon, C. S., I. Collins, A. Dershowitz, A. M. Deshpande, S. A. Greenfeder, L. Y. Ong, and J. F. Theis.** 1993. Analysis of replication origin function on chromosome III of *Saccharomyces cerevisiae*. Cold Spring Harbor Symp. Quant. Biol. **58:**415–423.
43. **Newlon, C. S. L. R. Lipchitz, I. Collins, A. Deshpande, R. J. Devenish, R. P. Green, H. L. Klein, T. G. Palzkill, R. B. Ren, S. Synn, and S. T. Woody** 1991. Analysis of a circular derivative of *Saccharomyces cerevisiae* chromosome III:

a physical map and identification and location of ARS elements. Genetics **129:**343–357.
44. **Okuno, Y., H. Satoh, M. Sekiguchi, and H. Masukata.** 1999. Clustered adenine/thymine stretches are essential for function of a fission yeast replication origin. Mol. Cell. Biol. **19:**6699–6709.
45. **Palacios DeBeer, M. A., and C. A. Fox.** 1999. A role for a replicator dominance mechanism in silencing. EMBO J. **18:**3808–3819.
46. **Palmer, B. R., and M. G. Marinus.** 1994. The *dam* and *dcm* strains of *Escherichia coli*—a review. Gene **143:**1–12.
47. **Palzkill, T. G., and C. S. Newlon.** 1988. A yeast replication origin consists of multiple copies of a small conserved sequence. Cell **53:**441–450.
48. **Palzkill, T. G., S. G. Oliver, and C. S. Newlon.** 1986. DNA sequence analysis of ARS elements from chromosome III of *Saccharomyces cerevisiae*: identification of a new conserved sequence. Nucleic Acids Res. **14:**6247–6264.
49. **Rao, H., Y. Marahrens, and B. Stillman.** 1994. Functional conservation of multiple elements in yeast chromosomal replicators. Mol. Cell. Biol. **14:** 7643–7651.
50. **Rao, H., and B. Stillman.** 1995. The origin recognition complex interacts with a bipartite DNA binding site within yeast replicators. Proc. Natl. Acad. Sci. USA **92:**2224–2228.
51. **Richterich, P., N. D. Lakey, H. M. Lee, J. I. Mao, D. Smith, and G. M. Church.** 1995. Cytosine specific DNA sequencing with hydrogen peroxide. Nucleic Acids Res. **23:**4922–4923.
52. **Rowley, A., J. H. Cocker, J. Harwood, and J. F. Diffley.** 1995. Initiation complex assembly at budding yeast replication origins begins with the recognition of a bipartite sequence by limiting amounts of the initiator, ORC. EMBO J. **14:**2631–2641.
53. **Shirahige, K., T. Iwasaki, M. B. Rashid, N. Ogasawara, and H. Yoshikawa.** 1993. Location and characterization of autonomously replicating sequences from chromosome VI of *Saccharomyces cerevisiae*. Mol. Cell. Biol. **13:**5043–5056.
54. **Sikorski, R. S., and P. Hieter.** 1989. A system of shuttle vectors and yeast host strains designed for efficient manipulation of DNA in *Saccharomyces cerevisiae*. Genetics **122:**19–27.
55. **Struhl, K., D. T. Stinchcomb, S. Scherer, and R. W. Davis.** 1979. High-frequency transformation of yeast: autonomous replication of hybrid DNA molecules. Proc. Natl. Acad. Sci. USA **76:**1035–1039.
56. **Theis, J. F., and C. S. Newlon.** 1997. The *ARS309* chromosomal replicator of *Saccharomyces cerevisiae* depends on an exceptional ARS consensus sequence. Proc. Natl. Acad. Sci. USA **94:**10786–10791.
57. **Theis, J. F., and C. S. Newlon.** 1994. Domain B of *ARS307* contains two functional elements and contributes to chromosomal replication origin function. Mol. Cell. Biol. **14:**7652–7659.
58. **Theis, J. F., C. Yang, C. B. Schaefer, and C. S. Newlon.** 1999. DNA sequence and functional analysis of homologous ARS elements of *Saccharomyces cerevisiae* and *S. carlsbergensis*. Genetics **152:**943–952.
59. **Van Houten, J. V., and C. S. Newlon.** 1990. Mutational analysis of the consensus sequence of a replication origin from yeast chromosome III. Mol. Cell. Biol. **10:**3917–3925.
60. **Vaughn, J. P., P. A. Dijkwel, L. H. Mullenders, and J. L. Hamlin.** 1990. Replication forks are associated with the nuclear matrix. NAR **18:**1965–1969.
61. **Vujcic, M., C. A. Miller, and D. Kowalski.** 1999. Activation of silent replication origins at autonomously replicating sequence elements near the *HML* locus in budding yeast. Mol. Cell. Biol. **19:**6098–6109.
62. **Walker, S. S., A. K. Malik, and S. Eisenberg.** 1991. Analysis of the interactions of functional domains of a nuclear origin of replication from *Saccharomyces cerevisiae*. Nucleic Acids Res. **19:**6255–6262.
63. **Wicksteed, B. L., I. Collins, A. Dershowitz, L. I. Stateva, R. P. Green, S. G. Oliver, A. J. Brown, and C. S. Newlon.** 1994. A physical comparison of chromosome III in six strains of *Saccharomyces cerevisiae*. Yeast **10:**39–57.
64. **Yamashita, M., Y. Hori, T. Shinomiya, C. Obuse, T. Tsurimoto, H. Yoshikawa, and K. Shirahige.** 1997. The efficiency and timing of initiation of replication of multiple replicons of *Saccharomyces cerevisiae* chromosome VI. Genes Cells **2:**655–665.
65. **Yang, C., J. F. Theis, and C. S. Newlon.** 1999. Conservation of ARS elements and chromosomal DNA replication origins on chromosomes III of *Saccharomyces cerevisiae* and *S. carlsbergensis*. Genetics **152:**933–941.